

## **Washington University in St. Louis Research**

The following report (which has been submitted as a topical report) from Washington University for the period April - June 1996 contains the following chapters:

1. Objectives
2. Summary
3. Appendix A: Two Phase Recycle with Cross Flow Model (TRCFM) for Gas Phase in Bubble Column Reactors (Task 3)
4. Appendix B: Progress in Understanding the Fluid Dynamics of Bubble Column Reactors (Task 6)

*Slurry Bubble Column Hydrodynamics*  
*Fifth Quarterly Report for Contract DOE-FC 22 95 PC 95051*

April - June 1996

Subcontract Objectives

This is the second year of the five year subcontract from the Department of Energy via Air Products. The main goal of this subcontract to the Chemical Reaction Engineering Laboratory (CREL) at Washington University is to study the fluid dynamics of slurry bubble columns and address issues related to scale-up. All the targets set for the first year including

- 1) review and recommendations of measurement techniques for multiphase flows with emphasis on the AFDU LaPorte reactor,
- 2) interpretation of the tracer studies from AFDU LaPorte reactor during methanol synthesis based on the axial dispersion model,
- 3) modifications of the CARPT/CT facility to accommodate studies in slurry systems,
- 4) development of a phenomenological model for liquid recirculation and
- 5) testing of closure schemes in CFD modeling)

have been met in a timely fashion. Two topical reports were submitted to Air Products: one on measurement techniques in multiphase flows, the other on interpretation of tracer studies in LaPorte AFDU during methanol synthesis based on the axial dispersion model.

For the second year of the contract the following objectives are set:

1. Complete review of gamma ray tomography and densitometry for obtaining density profiles with emphasis on applications in the LaPorte AFDU reactor.
2. Develop phenomenological models for liquid (slurry) and gas flow and mixing.
3. Use developed phenomenological models in interpretation of tracer runs at LaPorte.
4. Extend the CARPT/CT data base.
5. Continue the evaluation of closure schemes for CFD modeling.

It should be noted that objectives 4 and 5 are really coupled, and may have been previously reported as a single item, inasmuch that CARPT/CT data at different conditions is needed for evaluation of CFD codes.

We will now address progress made in accomplishing the above objectives and in summary present a PERT chart as to where we currently stand.

1. **Tomography**

Evaluation of relative merits of tomography and densitometry has been completed. The final topical report on this subject is in preparation and will be issued during the next quarter. It will contain information relevant to the AFDU LaPorte unit.

2. **Development of Phenomenological Models for Liquid and Gas Flow and Mixing**

A. **Liquid**

This model and its governing equations were presented in our 3rd quarterly report and will not be repeated here. The model is based on the experimentally observed steady single cell liquid recirculation pattern. It assumes that the upflow and downflow liquid stream communicate via an exchange coefficient (the physical basis for this is the turbulence created by bubble wakes). In addition, there is axial dispersion in each liquid region caused by wakes of small bubbles.

B. **Gas**

The gas phase model is developed based on the same physical picture as the liquid model and is described in detail in Appendix A of this report.

3. **Use of Phenomenological Models in Interpretation of Tracer Runs**

The liquid recirculation and crossflow and dispersion model (RCFD) outlined in the 3rd quarterly report was set up to predict tracer responses in the AFDU during methanol synthesis. The model and the methodology used are described in the enclosed paper prepared for the DOE Joint Power and Fuels Conference in Pittsburgh, July 1996 (see Appendix B). Additional details will be forthcoming in the follow-up reports.

4. **Extension of CARPT/CT Data Base**

Work continues, as mentioned in monthly reports, to provide data in a larger diameter 18" column. Results will be discussed in a subsequent reports.

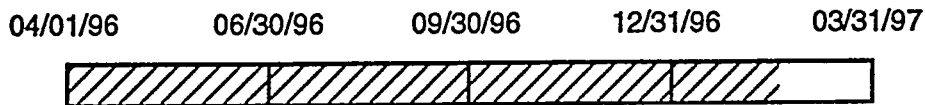
5. **Evaluation of Closure Schemes for CFD Modeling**

This computational effort continues. Comprehensive results will be reported upon completion of the study.

**SUMMARY**

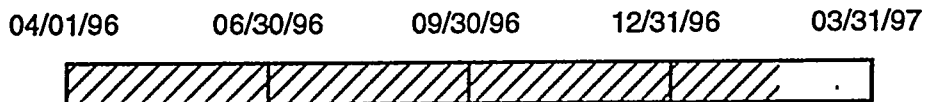
The chart below summarizes the objectives set for the 2nd year of the subcontract and illustrates where we are after the completion of the first quarter of year 2 (fifth quarter overall).

**1. Tomography**

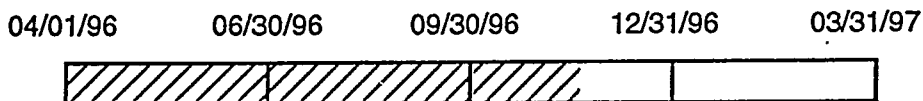


**2. Phenomenological Models**

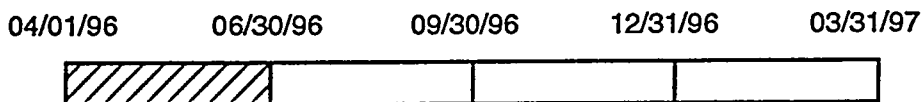
**2a. Liquid**



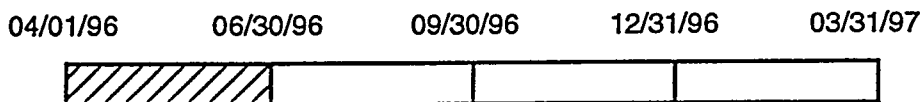
**2b. Gas**



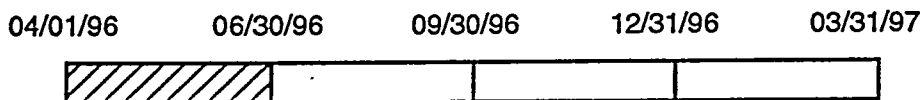
**3. Use of developed phenomenological models in tracer data (LaPorte) Interpretation**



**4. Extension of CARPT/CT Data Base**



**5. Evaluation of CFD Models**



## APPENDIX A

### A TWO PHASE RECYCLE WITH CROSS FLOW MODEL (TRCFM) FOR GAS PHASE IN BUBBLE COLUMN REACTORS

#### Introduction

The ultimate goal in bubble column research is to rapidly scale up from the laboratory size to pilot plant size and finally to industrial bubble column scale. It is known that gas and liquid phase mixing, turbulent intensity and residence time distributions are critical to the design, scale-up and operation. During the past two decades, modeling of the mixing behavior of both gas and liquid phases has been widely investigated but it is not yet completely successful. This is due to difficulties in describing the complexities of the liquid backmixing behavior, including chaotic phenomena and bubble size distribution in the churn turbulent regime either through experiments or via a theoretical approach. The difference in the behavior of large and small bubbles, the interaction among bubbles in churn turbulent regime due to coalescence and break-up of bubbles, and the coupling of the interphase mass transfer with chemical reactions also make predictive modeling very difficult.

Recently, interest has arisen in operating the bubble column reactors at very high gas superficial velocities, *i.e.*, in the churn-turbulent regime. In the churn turbulent regime, a bimodal bubble size distribution was assumed for the gas phase by Vermeer and Krishna (1981) and Shah and Joseph (1985). The flow in that regime becomes chaotic, and is characterized by fast moving large bubbles in the presence of small bubbles which are carried with the recirculated liquid. Gas phase mixing, which is an important hydrodynamic parameter to be considered in the scale-up of bubble columns, cannot be simply modeled by the axial dispersion model (ADM) in churn turbulent flow. Therefore, a new phenomenological model that relies on the realistic physical picture of bubble columns in the churn turbulent regime, and can fit the observed experimental residence time distribution (RTD) curves needs to be developed.

A single phase recycle with cross flow model (RCFM) was first developed in 1970 by Hochman and McCord and was successfully applied for tall tanks with a number of axial impellers. Myers et al (1986) and Degaleesan et al (1996) extended its application by successfully implementing the model to the liquid phase in bubble column reactors. Froment and Bischoff (1990) have also noted the applicability of this model to the bubble column system. Based on these findings, a recycle with cross flow type phenomenological model is proposed for both phases in the bubble column in this work. The model parameters are determined through experimental observations and empirical correlations.

#### Model Development

Based on the experimental observations of Hill (1974) and Devanathan et al (1990), large scale liquid circulation exists in bubble columns. The liquid ascends in the core region of the

column and descends in the annular region close to the wall, which results in the overall liquid circulation and forms what is called a "cell pattern". In the homogeneous regime, e.g. bubbly flow regime, only small bubbles of uniform size exist. These small bubbles, which are carried with the recirculated liquid, exhibit a slip velocity between the gas and the liquid. The motion of small bubbles in the bubbly flow regime may exhibit two distinct flow patterns. Small bubbles may rise in the core of the column or descend in the annular region close to the wall due to the downward velocity of liquid. Hence, gas recirculation is induced by liquid circulation, and there is interaction between the upflow of the liquid and the downflow of the liquid and between the upflow of the small bubbles and downflow of the small bubbles due to the shear stress between these two regions.

The heterogeneous regime, where the superficial gas velocity is high enough so that there is a distinct bimodal bubble size distribution, is usually called the 'churn turbulent regime'. In this regime, because of bubble coalescence and break-up, there is interaction not only between the bubbles of the same size but also among bubbles of different sizes. Due to the extreme complexities of bubble interaction and uncertainties regarding the bubble size distribution, two bubble sizes (large and small bubbles) are assumed here. Based on experimental observations, the large bubbles are assumed to rise in plug flow near the core region of the bubble column with higher velocity; the small bubbles, which are carried by the recirculated liquid, travel with lower velocity. The recirculation pattern of the small bubbles consists of upflow in the core region and downflow in the annular region. Figure I shows the typical flow diagram for small bubbles and liquid, the volume occupied by small bubbles, and the time averaged liquid velocity distribution in each region. Due to the shear between the upflow and the downflow of small bubbles and the liquid itself, it is assumed that interactions exist between the small bubbles in the two flow regions, as well as between the liquid in the two flow regions. These interactions are described via exchange coefficients. In addition, the exchange coefficient between the small and large bubbles is also defined in the model. This allows for the coalescence and break-up of the bubbles to be accounted for.

The proposed model may also be applied for the case where interfacial mass transfer is present such as for the gas component that is partially absorbed in the liquid or for a soluble gas tracer injected into the bubble column system. The mass transfer coefficients, representing transfer from both large and small bubbles to the liquid, are defined in the model to couple the phases. The model may also be applied for liquid phase chemical reactions when the reaction term is incorporated into the model equations.

Based on the above assumptions, a two phase recycle with cross flow model (TRCFM) is presented to physically describe gas and liquid phase mixing, various interaction among bubbles of the same and different sizes, between liquid in upflow and downflow regions, between gas and liquid phases in each region, as well as liquid phase reactions.

Figure 2. schematically represents the phenomenological basis for deriving the model equations for the two phase recycle with cross flow model (TRCFM). Thus, in the churn turbulent regime, the bubble column is assumed to be divided into nine different regions:

1. Large bubble upflow region (LB)
2. Small bubble upflow region (SB1)
3. Small bubble downflow region (SB2)
4. Liquid upflow region (L1)
5. Liquid downflow region (L2)
6. Distribution region for the gas phase in the inlet zone (GM1)
7. Disengagement region for the gas phase in the outlet zone (GM2)
8. Mixing zone of the liquid at the inlet of the bubble column (LM1)
9. Mixing zone of the liquid at the outlet of the bubble column (LM2)

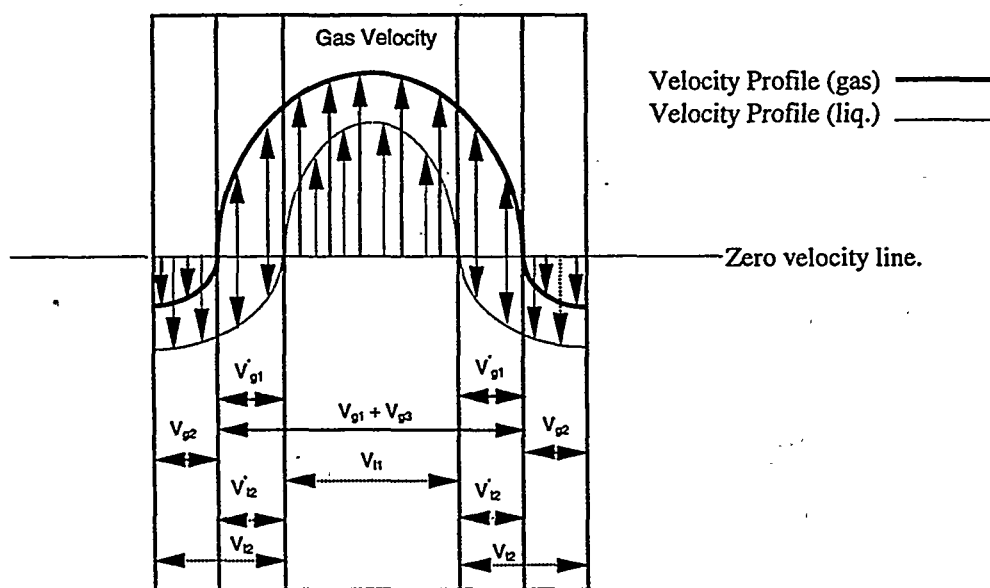


**FIGURE 1.** Schematic Diagram of Liquid and Gas Interstitial Velocity Profiles in Bubble Column Reactors

### Mathematical Model and Boundary Conditions

For the churn turbulent region, the proposed model is presented for two cases.

- 1) Continuous flow of both gas and liquid.
- 2) Batch liquid, continuous flow of gas.

#### I. Continuous flow of both gas and liquid

For the gas phase in small bubbles, the mass balance for a soluble gas component yields the equations for the various regions.

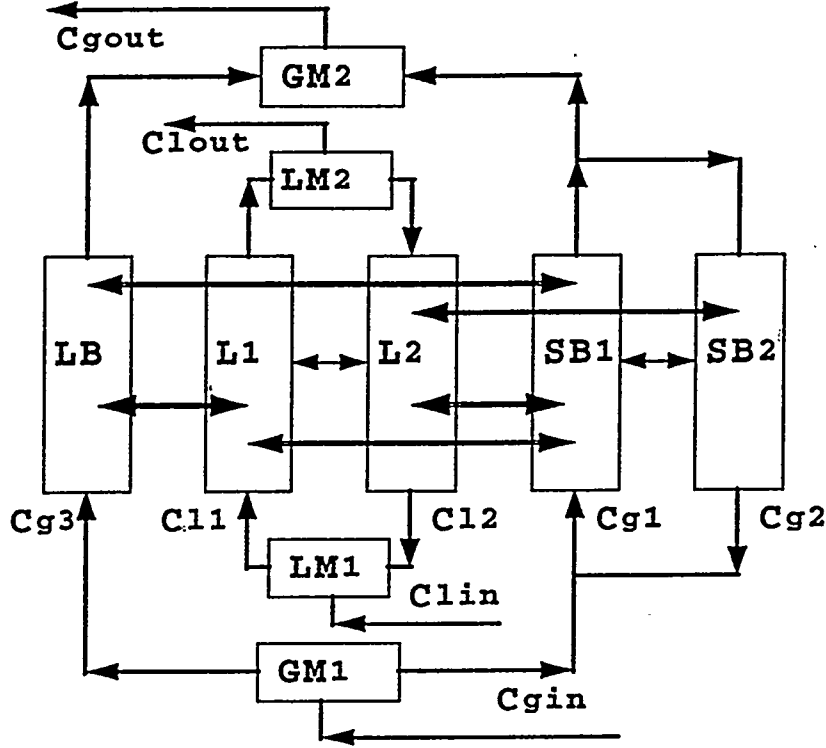


**FIGURE 2.** Schematic Diagram of TRCFM Model for Continuous Flow of Gas and Continuous Flow of Liquid

Upflow region of small bubbles ( SB1 )

$$\tau_{g1} \frac{\partial C_{g1}}{\partial t} + \frac{\partial C_{g1}}{\partial x} + \frac{K_{g12}}{1+r_{g12}} (C_{g1} - C_{g2}) + K_{g13} (C_{g1} - C_{g3}) - \left( \frac{V_{l1}}{V_{l1} + V_{l2}^1} \right) (k_{l1} a)^s (HC_{l1} - C_{g1}) \tau_{g1} - \left( \frac{V_{l2}^1}{V_{l1} + V_{l2}^1} \right) (k_{l2} a)^s (HC_{l2} - C_{g1}) \tau_{g1} = 0 \quad (1)$$

where  $r_{g12}$  is the recycle ratio for small bubbles, which is defined as the ratio of the gas volumetric flow rate to the SB2 region to the inlet volumetric flow rate of the gas into the small bubble region (SB1+SB2),  $V_{l1}$  and  $V_{l2}^1 (m^3)$  are, respectively, the volume of the liquid in the L1 section, and the volume of the liquid in that part of the L2 section where the interstitial velocity of small bubbles is greater than zero. (See Figure 2).

Downflow region of small bubbles (SB2)

$$\tau_{g2} \frac{\partial C_{g2}}{\partial t} - \frac{\partial C_{g2}}{\partial x} - \frac{K_{g12}}{r_{g12}} (C_{g1} - C_{g2}) - (k_{l2} a)^s (HC_{l2} - C_{g2}) \tau_{g2} = 0 \quad (2)$$

Upflow region of large bubbles (LB)

$$\tau_{g3} \frac{\partial C_{g3}}{\partial t} + \frac{\partial C_{g3}}{\partial x} - (k_l a)^l (HC_{l1} - C_{g3}) \tau_{g3} + K_{g13} (C_{g3} - C_{g1}) = 0 \quad (3)$$

The mass balance for a soluble gas component in the liquid phase yields the following equations for the various regions in the liquid phase.

Upflow region of liquid (L1)

$$\left[ \begin{array}{l} \tau_{l1} \frac{\partial C_{l1}}{\partial t} + \frac{\partial C_{l1}}{\partial x} + \frac{K_{l12}}{1+r_{l12}} (C_{l1} - C_{l2}) + \frac{V_{g1} - V_{g1}^1}{V_{l1}} \left( \frac{V_{g1} - V_{g1}^1}{V_{g3} + V_{g1} - V_{g1}^1} \right) (k_l a)^s \\ (HC_{l1} - C_{g1}) \tau_{l1} + \frac{V_{g3}}{V_{l1}} \left( \frac{V_{g3}}{V_{g3} + V_{g1} - V_{g1}^1} \right) (k_l a)^l (HC_{l1} - C_{g3}) \tau_{l1} + R_{l1} \tau_{l1} \end{array} \right] = 0 \quad (4)$$

where  $r_{l12}$  is the recycle ratio for the liquid which is defined as the ratio of the liquid volumetric flow rate of the L2 section to the inlet volumetric flow rate of liquid to the upflow and downflow liquid sections (L1+L2);  $V_{g1}, V_{g3}, V_{g1}^1$  ( $m^3$ ) are, respectively, the volumes of the small bubbles in SB1, the large bubbles in LB, and the volume of small bubbles in the section of the upflow region where the liquid goes downward (interstitial liquid velocity less than zero) and the small bubbles travel upward (interstitial gas velocity greater than zero);  $R_{l1}$  is the reaction term in the upflow region of the liquid. It is assumed that the reaction only occurs in the liquid phase.

In the liquid phase of the upflow region, as can be seen from Figures 1 and 2, one may encounter both large bubbles and small bubbles. In order to describe the contribution to mass transfer from large and small bubbles, a weighing function is defined based on the relative

volume percentage of small bubbles and large bubbles.  $\frac{V_{g1} - V_{g1}^1}{V_{g3} + V_{g1} - V_{g1}^1}$  is the weighing

factor for mass transfer contribution of small bubbles in the upflow section of the liquid, and

$\frac{V_{g3}}{V_{g3} + V_{g1} - V_{g1}^1}$  is the weighing factor for the contribution of large bubbles to mass transfer

in the upflow section of the liquid.

Downflow region of liquid (L2)

$$\left[ \begin{array}{l} \tau_{l2} \frac{\partial C_{l2}}{\partial t} - \frac{\partial C_{l2}}{\partial x} - \frac{K_{l12}}{r_{l12}} (C_{l1} - C_{l2}) + \frac{V_{g2}}{V_{l2}} \left( \frac{V_{g2}}{V_{g2} + V_{g1}^1} \right) (k_l a)^s \\ (HC_{l2} - C_{g2}) \tau_{l2} + \frac{V_{g1}^1}{V_{l2}} \left( \frac{V_{g1}^1}{V_{g2} + V_{g1}^1} \right) (k_l a)^s (HC_{l2} - C_{g1}) \tau_{l2} + R_{l2} \tau_{l2} \end{array} \right] = 0 \quad (5)$$

Here  $R_{l2}$  is the liquid phase reaction term in the downflow region of the liquid.

The downflow region of the liquid also may encounter either small bubbles in downflow or small bubbles in upflow (Figures 1 and 2). As discussed above for the liquid upflow region, weighing factors are defined for the relative contribution of small bubbles in upflow and small bubbles in downflow to mass transfer to the downward flowing liquid.  $\frac{V_{g2}}{V_{g2} + V_{g1}^1}$  is the

weighing factor for the contribution of small bubbles in downflow section, whereas  $\frac{V_{g1}^1}{V_{g2} + V_{g1}^1}$  is the weighing factor for the contribution of small bubbles in upflow section.

Initial conditions are presented in Equation 6 for a step injection of soluble tracer into the gas phase at the bottom of the bubble column, which is devoid of the injected gas component.

$t = 0$

$$C_{l1} = C_{l2} = C_{g1} = C_{g2} = C_{g3} = 0 \quad \text{and} \quad C_{g0} = H(t) \quad (6)$$

Boundary conditions are given by Equations 7 and 8 for the liquid and for the small bubbles at the bottom of the bubble column, and by Equations 9 and 10 for the large bubbles, small bubbles and the liquid at the top of the column.

$$x = 0 \quad C_{g1} = \frac{1}{1 + r_{g12}} (C_{g0} + r_{g12} C_{g2}) \quad (7)$$

$$C_{l1} = \frac{1}{1 + r_{l12}} (C_{l0} + r_{l12} C_{l2}) \quad (8)$$

$$C_{g3} = C_{g0} \quad (9)$$

$$x = 1 \quad C_{g1} = C_{g2}, \quad C_{l1} = C_{l2} \quad (10)$$

In deriving the above boundary conditions, it is assumed that the residence times in regions GM1, GM2, LM1 and LM2 (see Figure 1) are negligibly small, so that the mixing in the entry region and the disengagement zone is infinitely fast on the time scale of events occurring in the upflow and the downflow zones.

The total gas phase concentration at the outlet of the bubble column is given by:

$$C_{gout} = \frac{Q_{g12}}{Q_{g12} + Q_{g3}} C_{g1} + \frac{Q_{g3}}{Q_{g12} + Q_{g3}} C_{g3} \quad (11)$$

$$\text{or } C_{gout} = \frac{U_{g12}}{U_g} C_{g1} + \frac{U_{g3}}{U_g} C_{g3} \quad (12)$$

which assumes perfect mixing at the exit. It is assumed that for a step input of tracer (Heavisides step function at  $x = 0$ ), the solution of the model equations yields the F-curve, which on differentiating with respect to time yields an E-curve. Mathematically,

$$E(t) = dF/dt = dC/dt \quad (13)$$

At the outlet ( $x=1$ ),

$$E(t) = \frac{U_{g12}}{U_g} E_{SB}(t) + \frac{U_{g3}}{U_g} E_{LB}(t) \quad (14)$$

A normalized response, for a later comparison to experimental data, can be obtained by dividing  $E(t)$  in Equation 15 by its maximum value. Also, if necessary, the above model can be extended to account for finite time constants of the entry and disengagement regions as follows:

### The gas phase distributor zone (GM1)

Ideal mixer is assumed.

$$\tau_{gin} \frac{\partial C_g}{\partial t} = C_{gin} - C_{gout} \quad (15)$$

Negligible residence time is assumed in this section, therefore,

$$\tau_{gin} = 0 \quad (16)$$

$$C_{gin} = C_{gout} \quad \text{or} \quad C_{g0} = C_{g3_{x=0}} = C_{g12_{x=0}} \quad (17)$$

### The disengagement zone (GM2)

Ideal mixer is assumed.

$$\tau_{gout} \frac{\partial C_g}{\partial t} = C'_{gin} - C_{gout} \quad (18)$$

In the same way as in the distributor zone it is assumed

$$\tau_{gout} = 0 \quad (19)$$

$$C'_{gin} = C_{gout} \quad \text{or} \quad C'_{gin} = \frac{Q_{gi2}}{Q_{g12} + Q_{g3}} C_{g1} + \frac{Q_{g3}}{Q_{g12} + Q_{g3}} C_{g3} \quad (20)$$

Refer to Equation 11 and Equation 12.

### The liquid inlet zone (LM1)

Ideal mixer is assumed.

$$\tau_{lin} \frac{\partial C_l}{\partial t} = C_{lin} - C'_{lout} \quad (21)$$

Negligible residence time is assumed in this section, therefore,

$$\tau_{lin} = 0 \quad (22)$$

$$C_{lin} = C'_{lout} \quad \text{or} \quad C_{l0} = C_{l12,x=0} \quad (23)$$

### The liquid outlet zone (LM2)

Ideal mixer is assumed.

$$\tau_{lout} \frac{\partial C_l}{\partial t} = C'_{lin} - C_{lout} \quad (24)$$

In the same way as in the distributor zone, it is assumed

$$\tau_{lout} = 0 \quad (25)$$

$$C'_{lin} = C_{lout} \quad \text{or} \quad C_{l1,x=1} = C_{l2,x=1} = C_{lout} \quad (26)$$

## II. Continuous flow of gas and batch liquid

In this case, the net flow rate of liquid is zero, the model equations are similar to the previous case, the only difference arises in the model equations for the liquid phase and in the inlet

boundary conditions which are presented below. The mass balance for the two liquid regions (L1 and L2) is now given as follows:

Upflow region of liquid (L1)

$$\left[ \begin{array}{l} \tau_{11} \frac{\partial C_{11}}{\partial t} + \frac{\partial C_{11}}{\partial X} + K'_{112}(C_{11} - C_{12}) + \frac{V_{g1} - V_{g1}^1}{V_{11}} \left( \frac{V_{g1} - V_{g1}^1}{V_{g3} + V_{g1} - V_{g1}^1} \right) (k_1 a)^s \\ (HC_{11} - C_{g1})\tau_{11} + \frac{V_{g3}}{V_{11}} \left( \frac{V_{g3}}{V_{g3} + V_{g1} - V_{g1}^1} \right) (k_1 a)^l (HC_{11} - C_{g3})\tau_{11} + R_{11}\tau_{11} \end{array} \right] = 0 \quad (27)$$

Downflow region of liquid (L2)

$$\tau_{12} \frac{\partial C_{12}}{\partial t} - \frac{\partial C_{12}}{\partial X} - K'_{112}(C_{11} - C_{12}) + \frac{V_{g2}}{V_{12}} \left( \frac{V_{g2}}{V_{g2} + V_{g1}^1} \right) (k_1 a)^s (HC_{12} - C_{g2})\tau_{12} + \frac{V_{g1}^1}{V_{12}} \left( \frac{V_{g1}^1}{V_{g2} + V_{g1}^1} \right) (k_1 a)^s (HC_{12} - C_{g1})\tau_{12} + R_{12}\tau_{12} = 0 \quad (28)$$

The boundary conditions at the bottom of the bubble column are given by the Equation 29 which reflects the absence of the fresh liquid feed.

$$x=0, \quad C_{11} = C_{12}, \quad C_{g1} = \frac{1}{1+r_{g12}}(C_{g0} + r_{g12}C_{g2}), \quad C_{g3} = C_{g0} \quad (29)$$

For the case of the bubbly flow regime, only small bubbles exist and the equations can be simplified accordingly. In Equation 1, the interaction term between the large bubbles and small bubbles is neglected. Equation 3 is neglected because of uniform small bubble size distribution. In Equation 4, the mass transfer term between the large bubbles and liquid is neglected. In the boundary conditions, Equation 9 is neglected.

Future Work

1. Show how to determine all the parameters in the proposed model.
2. Compute the tracer response using implicit finite difference with backward differences.
3. Apply the model to experimental data from bubble columns of different sizes.

Nomenclature

a = interfacial area ( $m^2/m^3$ )

$C$  = concentration ( $\text{mol}/\text{m}^3$ )  
 $H$  = Henry's constant  
 $H(t)$  = Heavside's step function  
 $k_e$  = exchange coefficient ( $\text{m}^2/\text{s}$ )  
 $k_l$  = mass transfer coefficient ( $\text{m}/\text{s}$ )  
 $K$  = dimensionless crossmixing coefficient in continuous-liquid-flow case  
 $K'$  = dimensionless crossmixing coefficient in batch-liquid case  
 $L$  = column height ( $\text{m}$ )  
 $Q$  = volumetric flow rate ( $\text{m}^3/\text{s}$ )  
 $r$  = recycle ratio  
 $t$  = time ( $\text{s}$ )  
 $U$  = superficial velocity ( $\text{m}/\text{s}$ )  
 $V$  = volume ( $\text{m}^3$ )  
 $x$  = dimensionless position in longitudinal direction

### Greek letters

$\varepsilon$  = gas hold up  
 $\bar{\varepsilon}$  = average gas hold up  
 $\tau$  = residence time (sec)

### Subscript

$b$  = bubble  
 $g$  = gas  
 $gl$  = large bubble  
 $gs$  = small bubble  
 $g_{in}$  = inlet of gas  
 $g_{out}$  = outlet of gas  
 $g_1$  = small bubble in upflow region  
 $g_{12}$  = between upflow and downflow of small bubbles  
 $g_{13}$  = upflow of small bubble and upflow of large bubble  
 $g_2$  = small bubble in downflow region  
 $g_3$  = large bubble in upflow region  
 $l$  = liquid  
 $l_{in}$  = inlet of liquid  
 $l_{out}$  = outlet of liquid  
 $LB$  = large bubble  
 $l_1$  = liquid in upflow region  
 $l_{12}$  = between upflow and downflow of liquid  
 $l_2$  = liquid in downflow region

large = large bubble

s = small bubble

SB = small bubble

### Superscript

l = large

s = small

### Bibliography

- (1) Field, R.W. and Davidson, J.F. 1980. *Axial dispersion in bubble columns*. Trans I Chem E, 58:228.
- (2) Towell, G.D. and Ackerman, G.H. 1972. *Axial mixing of liquid and gas in large bubble reactors*. 5th European International Symposium Chem. React. Eng., B3-1, Elsenz, Amsterdam.
- (3) Kawaoe, M., Otake, T. and Robinson, R.D. 1988. *Gas phase mixing in bubble column*. Journal of Chem Eng. of Japan. 22 (2): 136-142.
- (4) Van Vuuren, D. S. 1988. *The transient response of bubble columns*. Chem. Eng. Sci. 43 (2): 213-220.
- (5) Shetty, S.A., Kantak, M.V. and Kelkar, B.G. 1992. *Gas-phase backmixing in bubble-column reactors*. AIChE. J. 38(7): 1013-1026.
- (6) Modak, S. Y., Juvekar, V.A. and Rane, V.C. 1993. *Dynamics of the gas phase in bubble column*. Chem. Eng. Technol. 16: 303-306.
- (7) Toseland, B.A., Brown, D.M., Zou, B.S. and Dudukovic', M.P. 1994. *Flow patterns in a slurry bubble column reactor under reaction conditions*. Trans. I. Chem. E. 73:297-301.
- (8) Myers, K.J., Dudukovic', M.P. and Ramachandran, P.A. 1986. *Modeling of churn-turbulent bubble columns 1: Liquid phase mixing*. Chem. Eng. Sci. 42:2301-2311.
- (9) Degaleesan, S., Roy, S., Kumar, S.B. and Dudukovic', M.P. 1996. *Liquid mixing based on convection and turbulent dispersion in bubble columns*. Accepted at the 14th Chem React. Eng. Conference.
- (10) Levenspiel, O. and Fitzgerald, T.J. 1983. *A Warning on the misuse of the dispersion model*. Chem. Eng. Sci. 38(3):489-491.

- (11) Deckwer, W.D. and Schumpe, A. 1993. *Improved tools for bubble column reactor design and scale-up*. Chem. Eng. Sci. 48:889-911.
- (12) Lubbert, A. and Larson, B. 1990. *Detailed investigations of the multiphase flow in airlift tower loop reactors*. Chem. Eng. Sci. 45 (10):3047-3053.
- (13) Devanathan, N., Moslemian, D. and Dudukovic', M.P. 1990. *Flow mapping in bubble columns using CARPT*. Chem. Eng. Sci. 45:2285-2291.
- (14) Vermeer, D.J. and Krishna, R. 1981. *Hydrodynamics and mass transfer in bubble columns operating in the churn-turbulent regime*. Ind. Eng. Chem. Proc. Des. Dev. 20:475-482.
- (15) Shah, Y.T. and Joseph, S. 1986. *Errors caused by tracer solubility in the measurement of gas phase axial dispersion*. Can. J. Chem. Eng. 64:380.
- (16) Hochman, J.M. and McCord, J.R. 1970. *Residence time distribution in recycle systems with crossmixing*. Chem. Eng. Sci. 25:97-107.
- (17) Froment, G.F. and Bischoff, K.B. 1990. *Chemical Reactor Analysis and Design*. 2nd ed; John Wiley and Sons: New York, 543-547.
- (18) Hill, J.H. 1974. *Radial non-uniformity of velocity and voidage in a bubble column*. Trans. Inst. Chem. Engrs. 52:1-9.
- (19) Wang, Q. and Dudukovic', M.P. 1996. *A two phase recycle with cross flow model for churn turbulent bubble columns*, presented in the 5th World Congress of Chemical Engineering. July 14-18, 1996
- (20) Wang, Q. 1996. *Modeling of gas and liquid phase mixing with reactions in bubble column reactors*, MS Thesis, Washington University, St. Louis, MO.

## APPENDIX B

### Progress in Understanding the Fluid Dynamics of Bubble Column Reactors

*Presented at the First Joint Power & Fuels System Contractors Conference,  
Pittsburgh, July, 1996*

#### Abstract

Bubble columns and bubble column slurry reactors, due to their superior heat transfer characteristics, are the contactors of choice for conversion of syngas to fuels and chemicals. Improved understanding is needed for rational, more reliable scale-up and operation. The multiphase fluid dynamics of gas-liquid and gas-liquid-solid mixtures in these systems, which determine the mass and heat transfer and, hence, greatly affect reactor volumetric productivity and selectivity. Our focus here is on illustrating how recent measurements of flow patterns in these systems, achieved through the DOE sponsored hydrodynamics initiative, can provide a rational explanation for the observed tracer tests in operating units which is not achievable by the use of the conventional axial dispersion model.

#### Introduction

There are considerable reactor design and scale-up problems associated with natural gas conversion technologies which arise due to the special characteristics of these processes. Generally, large gas throughputs must be handled necessitating large diameter reactors; high pressure is required for good mass transfer, rates and volumetric productivity; large reactor heights are needed to reach high conversions. Finally, heat removal is often a problem due to the high exothermicity of the processes involved. Bubble columns and slurry bubble columns have emerged as leading candidates for a variety of gas conversion processes (Krishna et al., 1996).. Successful commercialization of these new technologies is greatly dependent on the proper understanding of multiphase fluid dynamics in these systems. Due to complex flow patterns in bubble columns the design and scale-up of these reactors poses a rather difficult problem, and has so far been based on empiricism and on ideal reactor models (e.g. plug flow of gas, complete backmixing of liquid) or their simple extensions (e.g. axial dispersion model for gas and liquid).. In recent years considerable effort has been made to obtain a fundamentally based description of multiphase fluid dynamics in bubble columns (Svendsen et al., 1992, 1993, 1996, Sokolichin and Eigenberger, 1995). However, the uncertainty regarding the phase interaction terms and turbulence closure schemes, as well as problems associated with computation of large flow fields, have delayed the implementation of these models in practice.

The Department of Energy sponsored initiative for multiphase hydrodynamics attempts to fill the gap by providing the needed high quality data for testing of multiphase fluid dynamic codes. The interactive effort between Ohio State University (OSU), Washington University (WU) and Air Products (AP) has the ultimate goal of establishing predictive computational fluid dynamics (CFD) codes which can be used for scale-up and design. Currently, the CFD Library of Los Alamos (Kashiwa - year) is being examined as a possible candidate. The CFD codes still require the user to supply a physical model for phase interactions and turbulence. In order to examine the variety of possibilities for such models, code predictions must be compared to reliable data for the velocity and holdup field. Unique and sophisticated instrumental techniques have been developed and dedicated to that task at both universities involved in this project. At OSU, Particle Image Velocimetry (PIV) is used to obtain instantaneous velocity and holdup fields in selected planes within the column from which turbulence parameters can be calculated (Fan at OSU). At WU Computer Aided Radioactive Particle Tracking (CARPT) is used to monitor particle trajectories throughout the column and from these obtain instantaneous and time averaged velocities, turbulence and backmixing parameters (Yang, et al, 1993), while Computed Tomography (CT) is applied to get time averaged holdup distributions in various cross-sections of the column (Kumar et al., year). In addition, investigation of various local probes for heat transfer, local holdup and local velocity measurement is also in progress. At AP the overall behavior of the operating AFDU unit in LaPorte is monitored and characterized via pressure drop, gamma densitometry and gas and liquid tracer studies. Here, we describe how the measurements made at the universities have allowed us to develop an improved phenomenological model for interpretation of tracer data obtained on the operating AFDU in LaPorte. Such a phenomenological model for liquid mixing is an important interim step in addressing the ability to assess reactor productivity, selectivity and bed removal rates.

### Liquid Backmixing in Bubble Columns

The usual assumption made by a design engineer is that the liquid in a slurry bubble column is perfectly mixed. Tracer runs confirm close to complete backmixing. However, the small departure from complete backmixing observed in Figure 1 can lead to significant differences in required reactor size. For example, for a second order reaction and over 98% required conversion the size of a CSTR would be over 20 times larger than that of the actual reactor exhibiting the residence time distribution (RTD) of Figure 1. Hence, the use of conservative design may lead to prohibitive capital expenditures. As a usual remedy in arriving at more realistic reactor sizes the axial dispersion model (ADM) is used. While ADM can usually match the observed tracer response exceedingly well ( $D = 258 \text{ cm}^2/\text{s}$  for Figure 1), the calculated Peclet number is low (less than unity) pointing to the lack of

a physical basis for the ADM. Due to the broadness of the RTD, selectivity in nonlinear processes can vary greatly depending on the micromixing at hand. Since prediction of axial dispersion coefficients in bubble columns for scale-up has not been a successful art (Fan, 1989), and since the ADM does not provide information on the nature of the micromixing in the system, alternatives to it must be sought.

Extensive studies utilizing CARPT have revealed that in a time averaged sense, large scale liquid circulation exists in the form of a recirculation cell, which occupies most of the column, height wise, with liquid ascending along the central core region and descending along the annular region between the core and the walls. While a single one dimensional velocity profile is always identified in this recirculation cell, which is in the middle part of the column (Devanathan et al., 1995; Duduković and Devanathan, 1993; Duduković et al., 1991), axial variations and secondary circulation are evident in the distributor and free surface region. However, the instantaneous flow pattern in these systems is far more complex with spiraling motion of the gas bubbles, and gas-liquid interaction leading to intense turbulence (Devanathan et al., 1995). Mixing of the liquid phase is therefore primarily due to convective liquid recirculation and turbulent dispersion due to bubble caused turbulence. The model presented below phenomenologically accounts for the contributions of liquid recirculation and turbulent interaction in describing liquid mixing. This model is an extension of the description employed by Wilkinson et al. (1993), who used simplifying assumptions for liquid velocities and holdups to analyze the effects of increased pressure on the liquid axial dispersion coefficient. It can also be considered to represent a continuous version of the discrete cell model of Myers et al. (1987).

### Recycle (Recirculation) and Cross Flow with Dispersion (RCFD) Model

The RCFD model, which relies on the experimental observations discussed above to describe liquid mixing in an axisymmetric system is shown in Figure 2. The bubble column is divided axially into three sections, a middle region and two end zones where the liquid turns around. For simplicity the end zones are assumed to be perfectly mixed. In the middle region liquid mixing is described by taking into account the recirculation of the liquid. This is done by dividing this region into two sections: one with liquid flowing up in the middle or core section 1 and another with liquid flowing down in the annulus between the core and the walls (section 2). The flow within each of these sections is assumed to be fully developed. This assumption is based on experimental observations of the liquid flow patterns obtained from CARPT in our laboratory as discussed above. Superimposed on this convective recirculation is the mixing caused by the random turbulent fluctuating motion of the fluid elements, induced by the wakes of the rising bubbles, which gives rise to axial dispersion as well as radial exchange between the two flow sections. Turbulent axial mixing is accounted for by an axial dispersion coefficient in each section, and radial mixing is incorporated into an exchange coefficient between section 1 and section 2.

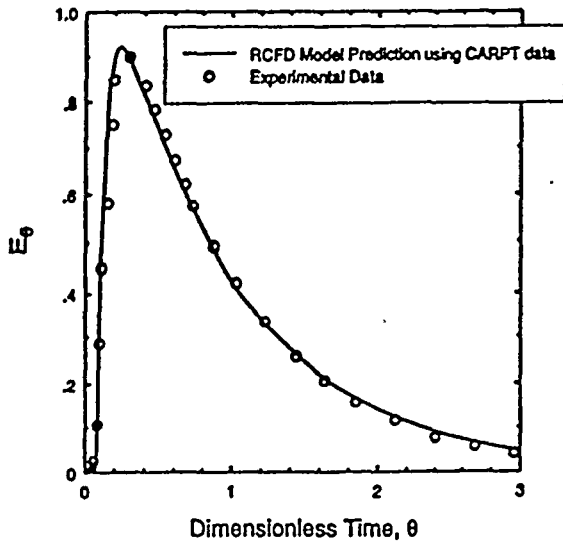


Figure 1: RTD curve from Myers et al. (1987)

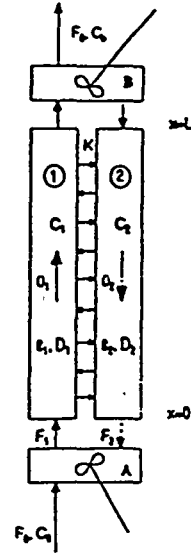


Figure 2: Schematic Diagram for the Recirculation and Cross Flow with Dispersion (RCFD) Model

Based on the above assumptions the model equations can be written as follows:

For the upflow region:

$$\frac{\partial C_1}{\partial t} = D_1 \frac{\partial^2 C_1}{\partial x^2} - \bar{u}_1 \frac{\partial C_1}{\partial x} - \frac{K}{A_1} (C_1 - C_2) \quad (1)$$

where  $K$  is the exchange coefficient ( $\text{cm}^2/\text{s}$ ), between the upflow and downflow sections.  $D_1$  is the axial eddy dispersion coefficient in the upflow region (section 1) based on the liquid covered cross sectional area, and  $\bar{u}_1$  and  $A_1$  are the average velocity, and the cross sectional area of the upflow section.  $C_1$  and  $C_2$  are the concentrations in section 1 and 2, respectively.

Similarly for the downflow region:

$$\frac{\partial C_2}{\partial t} = D_2 \frac{\partial^2 C_2}{\partial x^2} + \bar{u}_2 \frac{\partial C_2}{\partial x} + \frac{K}{A_2} (C_1 - C_2) \quad (2)$$

where  $D_2, \bar{u}_2, A_2$  are the axial eddy diffusivity, liquid velocity and cross-sectional area of region 2.

The equations for the well mixed regions, A and B which are assumed to be connected to the ends of the recirculating sections, are, respectively:

$$V_a \bar{E}_a \frac{\partial C_a}{\partial t} = F_0 C_0 - F_1 C_a + F_2 C_2 |_{x=0} \quad (3)$$

$$V_b \bar{\epsilon}_b \frac{\partial C_b}{\partial t} = F_1 C_1|_{x=L} - F_2 C_b - F_0 C_b \quad (4)$$

where  $F_0$  is the inlet liquid volumetric flow rate to the column and  $F_1$  and  $F_2$ , are the liquid volumetric flowrates in the upflow section 1 and downflow section 2.  $V_a$  and  $V_b$  are the volumes and  $\bar{\epsilon}_a, \bar{\epsilon}_b$  the average liquid holdup in the two regions. The initial conditions for a step input of tracer at the bottom of the column are:

$$C_0 = H(t) \quad \text{and} \quad C_1 = C_2 = C_a = C_b = 0 \quad @ \quad t = 0 \quad (5)$$

Danckwerts boundary conditions are used at the inlet of each section with no flux conditions at the outlet. Based on experimental observations, the heights of the two well mixed regions A and B are assumed to be equal to the diameter of the column.

The average upflow and downflow liquid interstitial velocities and holdups, which are required by this model, are provided as empirical input for each condition of interest. This experimental information is obtained by CARPT-CT measurements. The mean liquid velocities are calculated by cross sectional averaging of the recirculating liquid velocity profile obtained from CARPT measurements. The mean liquid holdup profiles are similarly obtained from CT measurements. In addition to obtaining the time averaged flow parameters, the velocity data from CARPT is used to evaluate the local radial,  $D_{rr}$ , and axial,  $D_{zz}$ , eddy diffusivities. An average value for  $D_{zz}$  is used for the upflow and for the downflow region (variation around these values is modest). The cross-flow exchange coefficient,  $K$ , is taken to be equal to the radial eddy diffusivities at the inversion plane.

In the CARPT technique a single neutrally buoyant radioactive particle, emitting  $\gamma$  radiation, is used to track the motion of the liquid phase. The radiation emitted by the particle is detected by an array of (NaI) scintillation detectors from which the position of the particle is calculated as a function of time. Time differencing of the subsequent positions results in instantaneous Lagrangian velocities, which are ensemble averaged to yield the time averaged velocities of the liquid phase at various locations in the entire domain of flow (Devanathan, 1991). The scanner for Computed Tomography, CT, (Kumar, 1995) is a transmission type scanner and is capable of obtaining the cross-sectional time averaged distribution of holdup in a two phase flow system. Since the cross-sectional void fraction distributions obtained in bubble columns are most often axisymmetric, the distribution can be circumferentially averaged to obtain radial void fraction profiles.

### Experimental Results

The tracer response data shown in Figure 1 is from Myers et al. (1987). The tracer experiment was

conducted in a 19 cm diameter column, with a gas superficial velocity of  $U_g = 10$  cm/s and a liquid superficial velocity of  $U_l = 1$  cm/s in an air-water system. The height of the column is 2.44 m and the mean residence time of the liquid was reported as 3.25 min. CARPT-CT experiments were conducted under identical conditions to obtain hydrodynamic data for this tracer experiment. The time averaged liquid velocity and holdup profiles obtained are shown in Figures 3 and 4, respectively, and are typical of previously reported results (Devanathan et al., 1990; Kumar et al., 1995). Gas holdup (one minus liquid holdup) is the highest in the center of the column and the lowest at the wall (Figure 4), which causes the highest upward liquid velocity in the center of the column and downward liquid flow by the walls (Figure 3), just as incorporated in our model. The mean liquid upflow and downflow velocities and corresponding holdups are computed using equation (6) and the following values are obtained:  $\bar{u}_1 = 12.5$  cm/s,  $\bar{u}_2 = 7.7$  cm/s,  $\bar{\epsilon}_1 = 0.79$  and  $\bar{\epsilon} = 0.88$ . An estimate of the axial eddy diffusivities in the upflow and downflow region is obtained by spatial averaging of the CARPT measured eddy diffusivities in the upflow and downflow section, respectively. These yield  $D_1 = D_{z_1} = 285$  cm<sup>2</sup>/s and  $D_2 = \bar{D}_{z_2} = 440$  cm<sup>2</sup>/s. The average value of the radial diffusivity at the point of velocity inversion is used as the estimate of the exchange coefficient  $K = \bar{D}_{rr,0} = 43$  cm<sup>2</sup>/s.

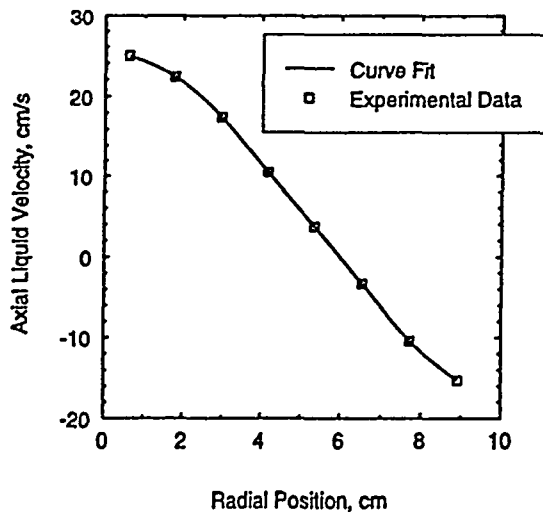


Figure 3: Azimuthally, Axially and Time averaged Liquid Axial Velocity Profile

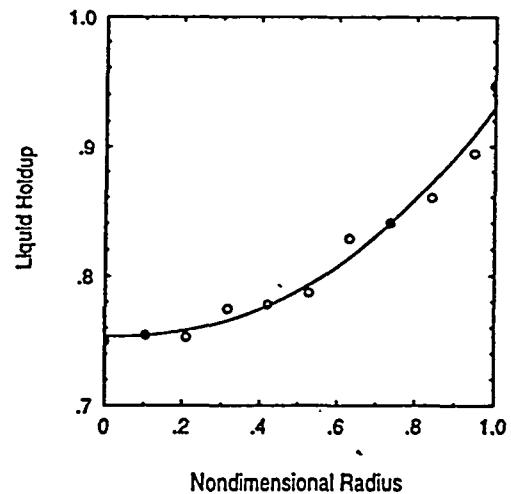


Figure 4: Azimuthally, Axially and Time Averaged Liquid Holdup Profiles

## Results and Discussion

Comparison of the model predicted impulse tracer response using CARPT-CT results for the dispersion coefficients, holdup and liquid velocities and the measured tracer response is also shown in Figure 1. The agreement is good which is remarkable since no free parameters are used to match the model calculated to the observed curve. This provides us with confidence that the RCFD model describes the mixing phenomena in the column well.

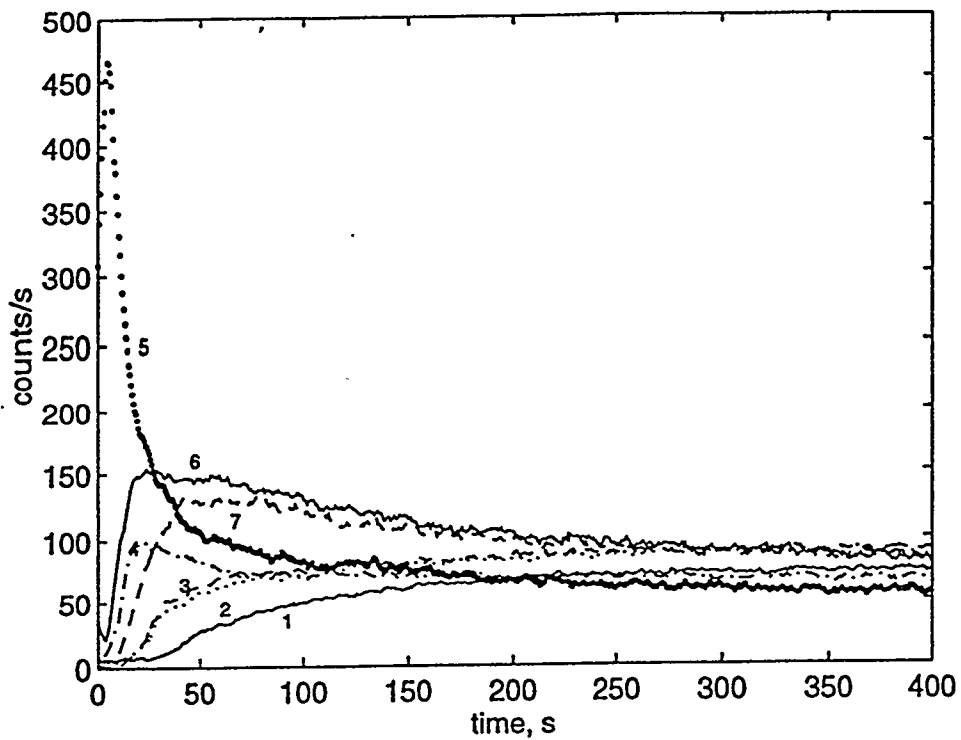


Figure 5: Experimental Tracer Responses in the LaPorte Reactor

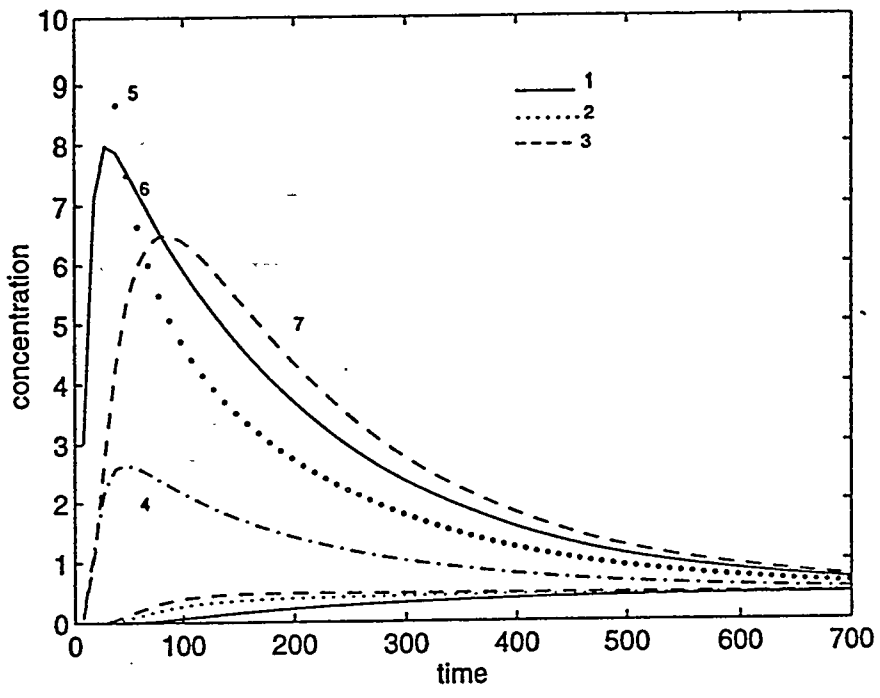


Figure 6: Model Calculated Responses at Detector Levels (similar to experiment), for qualitative comparison with Fig 5 (time scale is arbitrary)

Recent tracer studies conducted during liquid phase methanol (LPMEOH) synthesis runs in the AFDU oxygenates High Pressure Reactor at the LaPorte, Texas, confirm the inadequacy of the ADM and the promise of RCFDM. The unit is a 46 cm in diameter with liquid dispersion height of about 1300 cm. Liquid is in the batch mode and tracer is injected at various axial and radial locations (Figure 5). Tracer responses, subject to injection at N1 close to the wall, were measured at various levels (Figure 5) and cannot be interpreted based on the axial dispersion model which simply cannot predict the observed overshoots (or dependence on injection location, not shown). However, for the three detectors (1,2,3) furthest from the point of injection a monotonic response is observed and an axial dispersion coefficient, which is dependent on location of the detectors, can be obtained by fitting the ADM to the observed response. In contrast the RCFDM (Figure 6) exhibits semi-quantitatively the observed responses at all detector locations. The parameters used to calculate Figure 6 were obtained for a column of smaller diameter and at lower gas velocities. Nevertheless, the essence of the mixing pattern has been captured. How changes in diameter and pressure affect the liquid circulation pattern and eddy diffusivities is part of the future work, in order to obtain a more quantitative comparison of model predictions with experimental data.

## References

- Devanathan, N., Moslemian, D. and Duduković, M.P., 1990, Flow Mapping in Bubble Columns Using CARPT, *Chem. Engng. Sci.* **45**, 2285-2291.
- Devanathan, N., Duduković, M.P., Lapin, A. and Lubbert, A., 1995, Chaotic Flow in Bubble Column Reactors. *Chem. Engng. Sci.* **50**, 2661-2667.
- Devanathan, N., 1991, "Investigation of Liquid Hydrodynamics in Bubble Columns via Computer Automated Radioactive Particle Tracking (CARPT), D.Sc. Thesis, Washington University, St. Louis.
- Duduković, M., Devanathan, N. and Holub, R., 1991, Multiphase Reactors: Models and Experimental Verification. *Revue de l'Institut Francais du Petrole* **46**, 439-465.
- Duduković, M.P. and Devanathan, N., 1993, Bubble Column Reactors: Some Recent Developments, in *Chemical Reactor Technology for Environmentally Safe Reactors* (Edited by H.I. DeLasa, et. al), NATO ASI Series E: Appl. Sci. 225, 379-408.
- Fan, Liang-Shih, *Gas-Liquid-Solid Fluidization Engineering*. Butterworths, 1989.
- Grevskott, S., Sanneas, B.H., Duduković, M.P., Hjarbo, K.W. and Svendsen, H.F., 1996, Liquid Circulation, Bubble Size Distributions, and Solids Movement in Two- and three-phase Bubble Columns, *Che. Enng. Sci.* **51**, 1703-1714.
- Kashiwa, B.A. and Gore, R.A., 1991, A Four Equation Model for Multiphase Turbulent Flow.

Presented at the *First Joint ASME/JSME Fluids Engineering Conference*.

- Krishna, R., Ellenberger, J. and Sie, S.T., 1996, Reactor Development for Conversion of Natural Gas to Liquid Fuels: A Scale-up Strategy Relying on Hydrodynamic Analogies, *Chem. Engg. Sci.* **51**, 2041-2052.
- Kumar, S.B., Moslemian, D. and Duduković, M.P., 1995, A  $\gamma$  Ray Scanner for Imaging Voidage Distributions in Two Phase Flow Systems. *Flow Measurement and Instrumentation* **6**, 61-63, 1995.
- Myers, K.J., Duduković, M.P. and Ramachandran, P.A., 1986, Modeling of Churn-Turbulent Bubble Columns - I: Liquid Phase Mixing. *Chem. Engng. Sci.* **42**, 2301-2311.
- Sokolichin, A., Eigenberger, G., 1995, Gas-Liquid Flow in Bubble Columns and Loop Reactors: Part I. Detailed Modeling and Numerical Simulation. *Chem. Engng. Sci.* **49**, 5735-5746.
- Svendsen, H.F., Jakobsen, H.A. and Torvik, R., 1992, Local Flow Structures in Internal Loop and Bubble Column Reactors. *Chem. Engng. Sci.* **47**, 3299-3304.
- Wilkinson, P.M., Haringa, H. Stokman, F.P.A. and van Dierendonck, L.L., 1993, Liquid Mixing in Bubble Columns Under Pressure. *Chem. Engng. Sci.* **48**, 1785-1791.
- Yang, Y.B., Devanathan, N. and Duduković, M.P., 1993, Liquid Backmixing in Bubble Columns via Computer-Automated Radioactive Particle Tracking (CARPT). *Exp. Fluids* **16**, 1-9.

### Task 3.3 - Sparger Modeling

Initial work on developing an understanding of the importance of the sparger in a SBCR consists of the initiation of a literature search and preliminary meetings and discussions with Sandia, Ohio State and Washington University personnel to understand the framework for an experimental study. The complete analysis of the literature search awaits conclusion of detailed reading of the documents and the final step of developing a search strategy. This section is a preliminary report on the progress of the search and a summary of the presentation made at Sandia that was based on that work.

#### *Literature Search-Preliminary Results*

Twenty-six documents were found in a standard search<sup>1</sup>. A good review of the older literature is found in Decker (1), while Hebrard et al. (2) provide a more recent summary. Despite these summaries, no clear pattern emerges on the effect of a sparger on even a simple parameter like overall holdup for bubble columns. In addition, only one reference was found for a sparger change for systems with solids (3).

The effect of gas distributor and material properties on  $\epsilon_g$  [gas holdup] is complex (1). Large differences in holdup with sparger type are measured at low (<10 cm/sec) gas velocities. Much of the difference is explained by changes in the onset of transition or the presence of imperfect bubble flow (2). These issues may not be applicable to the high flow rates of the churn turbulent flow regime.

Most of the data pertain to water/air, which is a high surface tension system and may behave very differently from low surface tension organic systems. Most measurements are at or near atmospheric pressure. The effects of pressure and increased solids loading are unclear. In most cases, the effects of sparger differences diminish as flow rate increases. Commonly studied spargers, for example, sintered metal plates, porous plates and rubber diaphragms, are useful for developing information, but are not practical for industrial situations that use catalyst.

In summary, the literature can provide some insight into what parameters should be considered in sparger design. However, insufficient information is available for sparger

---

<sup>1</sup>Data bases searched and search strategy are given below.

Engineering Index, Chemical Engineering and Biotech. Abstracts, NTIS  
Databases

Sparg?(within 10 words of ) slurry (within 10 words of) bubble column? or  
reactor?; also  
gas inlet or intake and bubble column? or reactor?

and in a second search

Search terms: Sparging - keyword; plus bubble columns - keyword

design for industrial systems at high gas flow rates and elevated pressures. The major findings from the search are that good design methods do not exist, and additional experimental work is needed to begin to understand the importance of various sparger parameters on column performance.

### *Design Issues*

A sparger has only one function--introduction of gas to the reactor. However, gas distribution can influence the performance of the bubble column in several ways:

- bubble size distribution, which in turn can affect mass transfer
- radial bubble distribution, which is a measure of uniformity and, therefore, reactor utilization
- uniformity of solids distribution
- erosion of the vessel or internal walls

Thus, one must consider the method of bubble generation, as well as the type of distributor and its placement in the reactor in any study of the function of the distributor.

The objective of the experimental study will be to ascertain the importance of sparger design when the reactor is operating in the churn turbulent regime of slurry bubble column flow. It is clear that a single pipe sparger might not give adequate gas distribution. What is not clear is the importance of hole size in obtaining a uniform degree of mixedness in a SBCR. Similarly, uniform flow may not be achieved if the sparger is placed at the edge of the radius of the column, but the degree of maldistribution allowed while a uniform distribution is maintained is not at all clear. An initial sparger study should answer questions such as

- What is the importance of sparger hole size?
- What is the sensitivity of the degree of mixedness of the system to sparger placement?

In short,

- What degree of care must be taken to have a well-mixed system?

This study is intended to gain an understanding of what constitutes an adequate sparger system.

### *Bubble Formation*

In general, three conditions of bubble formation have been identified: a constant flow condition, a constant pressure condition, and a condition intermediate between the two. Somewhat surprisingly, the size of a bubble can depend upon the volume of the sparger chamber for the latter two cases (4). Bubble formation can be divided further by considering the gas flow rate. At high gas flow rates ( $N_w > 16$ , where  $N_w = BoFr^{0.5}$  and  $Bo = \rho D^2 g / \sigma$  and  $Fr = U^2 / Dg$ ), the dependence of bubble formation on the sparger chamber is minimized. This is especially true when the pressure drop across the hole is high relative to the pressure fluctuations in the bubble during formation. For the conditions typically found in the LaPorte reactor,  $N_w$  is greater than 16. This eases the design problem somewhat. However, laboratory studies should always be carried out in this region as well. This means careful planning of sparger hole size and gas flow rates so that even for the largest size holes being tested,  $N_w$  is greater than 16 and the pressure drop across the

orifice is high relative to the fluctuations during bubble formation so that bubble size factors can be isolated from the other changes made.

### *Sparger Type*

Spargers made from sintered plates and pipes, porous plates and flexible diaphragms have been used for most academic studies. However, the presence of the fine catalyst particles precludes using these types of spargers in a commercial reactor. Other sparger types, for example, rings, doughnuts and crosses, have been used sparingly in academic studies. However, since these types of spargers should provide a much better simulation of an actual industrial-scale sparger, they should be the primary devices. A device such as a porous plate, which gives uniform distribution, should, of course, be used when a comparison with complete uniformity is desired. Hole orientation, up or down, should also be considered as part of this initial study. Maldistribution can be simulated by blocking one-half or one-quarter of the area of such a device.

### *References*

1. Deckwer, W. D. Bubble Column Reactors, 1992, John Wiley and Sons, p. 170ff
2. Hebrard, G., Bastoul, D., Roustan, M. *Trans I Chem E*, Vol. 74 Part A, April 1966, p. 406ff.
3. Smith, G. B., Gamblin, B. R. and Newton, D. *Trans I Chem E*, Vol 73, Part A, August, 1995, p. 632 ff.
4. Tsuge, H. Hydrodynamics of Bubble Formation From Submerged Orifices in Encyclopedia of Fluid Mechanics, N. Chermisinoff, Gulf Publishing Co. 1986, p. 1931.